Nanostructures

DOI: 10.1002/anie.201400377

Directed Self-Assembly of DNA Tiles into Complex Nanocages**

Cheng Tian, Xiang Li, Zhiyu Liu, Wen Jiang, Guansong Wang, and Chengde Mao**

Dedicated to Professor George M. Whitesides on the occasion of his 75th birthday.

Abstract: *Tile-based self-assembly is a powerful method in DNA nanotechnology and has produced a wide range of well-defined nanostructures. But the resulting structures are relatively simple. Increasing the structural complexity and the scope of the accessible structures is an outstanding challenge in molecular self-assembly. A strategy to partially address this problem by introducing flexibility into assembling DNA tiles and employing directing agents to control the self-assembly process is presented. To demonstrate this strategy, a range of DNA nanocages have been rationally designed and constructed. Many of them can not be assembled otherwise. All of the resulting structures have been thoroughly characterized by gel electrophoresis and cryogenic electron microscopy. This strategy greatly expands the scope of accessible DNA nanostructures and would facilitate technological applications such as nanoguest encapsulation, drug delivery, and nanoparticle organization.*

Programmed DNA self-assembly is a promising approach for nanoconstruction.[1–3] There are two general approaches: 1) tile-based assembly: the use of a small set of unique DNA strands to assemble simple, repetitive, symmetric structures;[2,4–15] and 2) non-tile-based assembly: the use of a large number of unique DNA strands to assemble complex structures.[16–24] However, it remains a great challenge to assemble complex DNA nanostructures with a small set of unique DNA strands. Algorithmic self-assembly is one approach in this direction and has generated impressive structures,[25–27] but its generality remains to be demonstrated. Recently, carefully designed multitiles have been used to assemble Archimedean 2D patterns.[28] Herein, we report

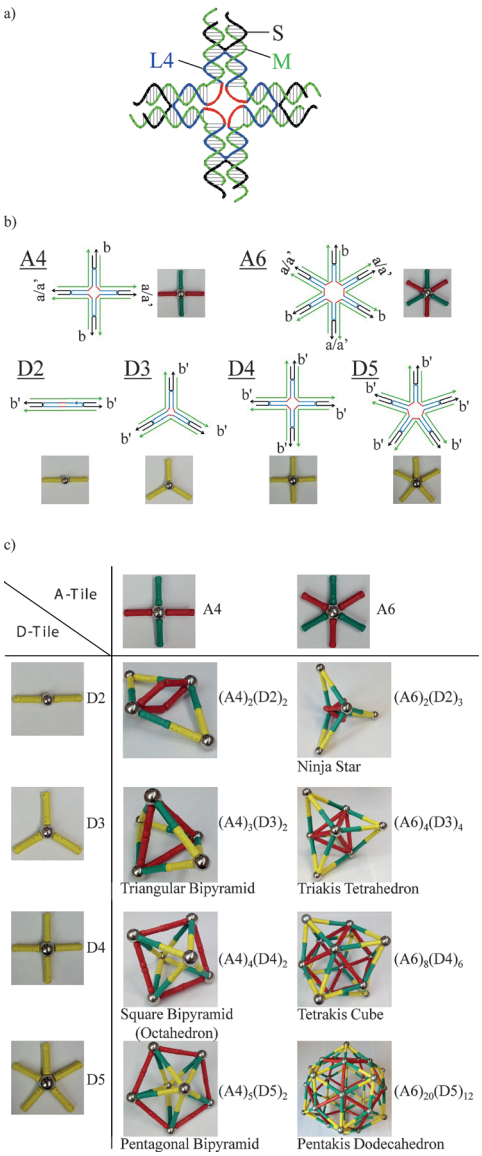

Figure 1. Directed self-assembly of DNA tiles. a) A detailed structure (prepared from Tiamat[29]) of a 4-point-star motif (tile) that exemplifies all of the tiles used. It consists of one L4 strand (blue/red), four M strands (green), and four S strands (black). b) Simplified schemes of the assembly tiles (A-tiles) and directing tiles (D-tiles). An *n*-point-star tile for an A- or D-tile is termed A*n* or D*n*, respectively. For each tile, a simple scheme indicating all of the component strands (lines with the same color coding as in Figure 1 a) and an even simpler ball and stick scheme are shown. The D*n* tile has an *n*-fold rotational symmetry and is assembled from three types of unique DNA strands: $L^{D}n$, M^{D}, and S^{D}. The A*n* tile has lower symmetry (an $\frac{n}{2}$-fold rotational symmetry) and is assembled from five types of DNA strands: $L^{A}n$, M^{A1}, M^{A2}, S^{A1}, and S^{A2}. The sticky ends a/a' are self-complementary and b and b′ are complementary to each other. c) A chart of the component tiles and the resulting DNA cages.

[*] C. Tian, X. Li, Z. Liu, Prof. C. Mao
Department of Chemistry, Purdue University
West Lafayette, IN 47907 (USA)
E-mail: mao@purdue.edu
Prof. W. Jiang
Markey Center for Structural Biology and
Department of Biological Sciences, Purdue University
West Lafayette, IN 47907 (USA)
Prof. G. Wang
Institute of Respiratory Diseases, Xinqiao Hospital
Chongqing 400037 (China)
E-mail: wanggs2003@hotmail.com

[**] We thank the Office of Naval Research and National Science Foundation for supporting this research. The cryo-EM images were taken in the Purdue Biological Electron Microscopy Facility.

Supporting information for this article is available on the WWW under http://dx.doi.org/10.1002/anie.201400377.

a directed DNA-tile self-assembly strategy to achieve moderately complex, symmetric 3D DNA nanostructures.

The reported strategy (Figure 1) uses two different types of DNA tiles: directing tiles (D-tiles) and assembly tiles (A-tiles). D-tiles are designed to direct the self-assembly of A-tiles and cannot associate with one another themselves. Each A-tile has two sets of sticky ends: one set is self-complementary, which allows A-tiles to assemble into large structures; the other set is complementary to the sticky ends of D-tiles and allows A-tiles to interact with and take instructions from D-tiles. A-tiles are intentionally introduced with sufficient flexibility and can adopt different conformations. In the absence of D-tiles, A-tiles will self-associate into a mixture of homo-oligomeric complexes with different sizes. In the presence of D-tiles, A-tiles are directed to form various complexes by and with different D-tiles.

All of the tiles used in this work are star-shaped motifs (tiles).[8,12,30–32] An *n*-point-star tile contains a central long strand ($L^D n$ for D-tiles and $L^A n$ for A-tiles; blue/red), *n* copies of the medium strands (M; green), and *n* copies of the short strands (S; black). At the center of the tile, there are *n* segments of single-stranded loops (red). The loop length positively correlates with the tile flexibility.[12,32] A D-tile with *n* branches, dubbed a D*n*-tile, has an *n*-fold rotational symmetry. And an A-tile with *n* branches, dubbed an A*n*-tile, has a lower, $\frac{n}{2}$-fold rotational symmetry. For any D-tile, all M strands (M^D) are the same and all S strands (S^D) are the same. Thus all branches, including the sticky ends (b′), are identical to one another. For the A-tiles, half of the M strands are M^{A1} and the other are M^{A2}. They alternate in the tile. The same applies to S strands: half are S^{A1} and half S^{A2}. Consequently, two types of sticky ends appear alternately at the branches of the A-tile: one (a/a′) is self-complementary and the other (b) is complementary to the sticky-end b' in the D-tile.

The assembly was carried out in a neutral Mg^{2+}-containing aqueous buffer by a thermal cooling process. Upon the completion of self-assembly, all of the DNA samples were initially analyzed directly by polyacrylamide gel electrophoresis (PAGE) or agarose gel electrophoresis (Figure 2, and Figures S1 and S2 in the Supporting Information). All of the D-tiles migrated fast as individual tiles without self-association; by contrast, the A-tiles formed a series of homo-oligomers with different sizes. In the presence of D-tiles, the A-tiles oligomerized into complexes with defined sizes determined by the D-tiles, thereby leading to a dominant sharp band in each lane with a high yield (estimated from the band intensities). In structures $[(A4)_2(D2)_2]$ or $[(A6)_2(D2)_3]$, the A-tiles were dramatically bent. Releasing such stresses leads to large aggregates and the assembly yields of the target structures became relatively low (68% and 58%, respectively). Complexes $[(A6)_8(D4)_6]$ and $[(A6)_{20}(D5)_{12}]$ were very large objects and could not easily penetrate into the PAGE matrix. They were trapped in the wells partially (for smaller the $[(A6)_8(D4)_6]$ complex) or completely (for the larger $[(A6)_{20}(D5)_{12}]$ complex). When agarose gels (with larger pores than the polyacrylamide gels) were used, both complexes migrated into the gel matrix as single bands.

To study the native 3D structures of the assembled DNA complexes, we applied cryogenic electron microscopy (cryoEM) to all of the DNA samples (Figures 3 and 4, and Figures S3-S17). Figure 3 and Figure S3 show the detailed cryoEM study of complex $[(A4)_5(D5)_2]$, a pentagonal bipyramid, and Figure 4 summarizes all of the assembled complexes. In the raw cryoEM image (Figure 3a), individual framework particles (indicated by white boxes) with the expected size are randomly distributed in the viewing field. From the observed individual particles, we have applied a technique of single-particle 3D reconstruction[33,34] to reveal the 3D structures of the DNA complexes. This technique revealed the structure of the expected pentagonal bipyramid at a resolution of 3.3 nm (Figure 3b). We have further compared the 2D projections calculated from the reconstructed model with 1) raw images of individual particles (Figure 3c) and 2) the class averages of raw particles at the same orientation (Figure S3). Clear similarity in the pairwise comparisons confirms that the reconstructed model truly represents the 3D structure of the self-assembled DNA complex. All of the other designs have also been confirmed by cryoEM studies with a moderate resolution (3.2–4.0 nm; Figure 4 and Figures S4–S17). The central cavities in 2- and 3-point star tiles are quite small and are not visible in the final structural models. By contrast, the 4-, 5-, and 6-point star tiles have larger cavities, which could be clearly seen.

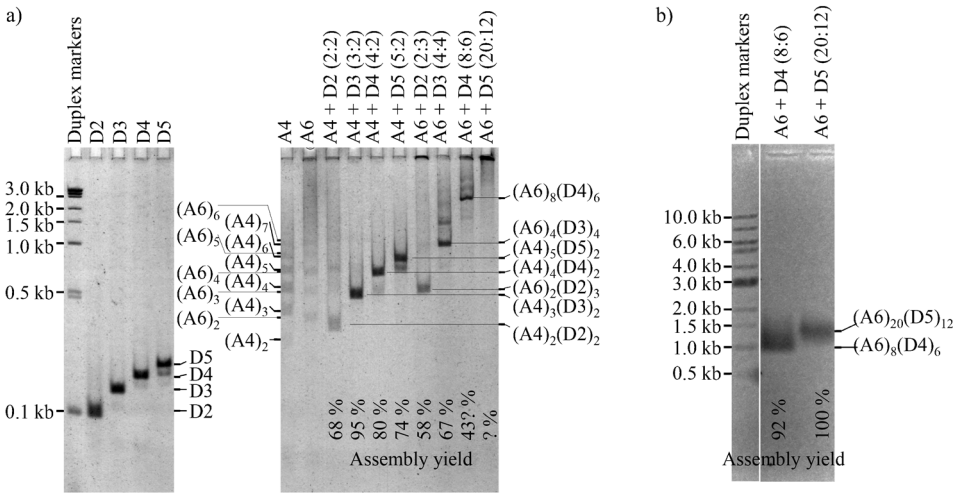

Figure 2. Analysis of directed DNA self-assembly by PAGE (a) and agarose gel electrophoresis (b). The sample compositions for each lane, the chemical identity of each band, and the assembly yields are shown above, beside, and below the gel images, respectively. The two images in Figure 2a are from one gel (Figure S1 in the Supporting Information) and the two parts in Figure 2b are from another gel (Figure S2).

Some previously reported DNA polyhedra, particularly

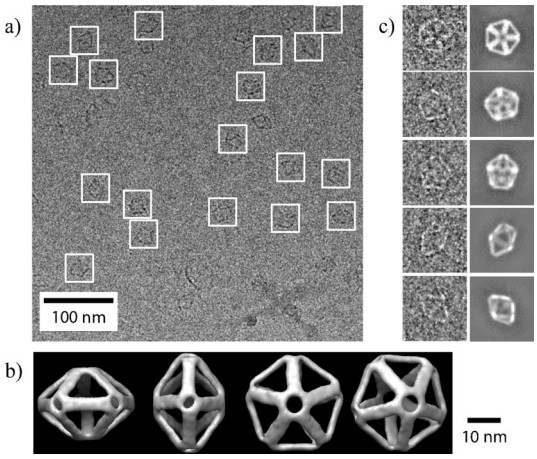

Figure 3. CryoEM study of pentagonal bipyramid [$(A4)_5(D5)_2$]. a) A representative cryoEM image. White boxes indicate the DNA complexes. b) Four views of the reconstructed structural model of the DNA pentagonal bipyramid. c) Pairwise comparison between raw cryoEM images of individual particles (left) and the corresponding projections (right) of the reconstructed structural model. The raw particles were selected from different image frames to represent views at different orientations.

the large ones such as dodecahedron and buckyball,[12] have non-triangular faces. This feature makes these polyhedra deformable. In the current study, all of the objects have triangular faces. Such geometry introduces rigidity to the polyhedra and makes them nondeformable.

The reported polyhedra can be classified into two families. 1) Simple bipyramids resulting from the A4 tile. The A4 tile by itself will assemble into circular oligomers. In the presence of D-tiles, those circular oligomers will be capped by the D-tiles from both the top and bottom and become the pyramid bases. 2) Complex polyhedra (Kleetopes of polyhedra) assembled from the A6 tile. This family of polyhedra can be viewed as face-capped regular polyhedra. Each object has a central, simple polyhedron, the face of which serves as the bottom of a pyramid.

In summary, we have demonstrated a directed self-assembly strategy to assemble large complex 3D structures, many of which have not been accessible before. For example, complex [$(A6)_{20}(D5)_{12}$] consists of twenty A6 tiles and twelve D5 tiles, totaling 16,020 bases. It has a molecular weight of approximately 5 megadaltons (MDa; Table 1), larger than a ribosome (ca. 2.8–4.0 MDa),[35] one of the most complicated biological machineries. It has a diameter of ~80 nm, comparable to most viruses (20–200 nm).[36] It is amazing that such a well-defined, large DNA complex can be readily assembled from only eight unique component sequences (475 bases in total). The current strategy mimics a natural biological process: the scaffolding-protein-assisted assembly of viral procapsids.[37–39] In many cases (e.g. bacteriophage P22), viral coat protein can correctly assemble into functional viral procapsids only in the presence of scaffolding proteins. Otherwise, they assemble into aberrant, smaller-than-normal cages. Such regulated molecular self-assembly offers a general approach for the precise construction of large, complex supramolecular structures. This work is also of interest for the study of molecular self-assembly and 3D nanofabrication, and for the preparation of nanodevices for biomedical and physical applications.

Table 1: Summary of the assembled DNA complexes: number of nucleotides, molecular weight, and overall dimensions.

Complex	Number of Nucleotides	Molecular Weight [Da]	Circumsphere Diameter [nm]
[$(A4)_2(D2)_2$]	1068	327857.6	32.2
[$(A4)_3(D3)_2$]	1602	491848.3	30.2
[$(A4)_4(D4)_2$]	2136	655715.2	27.2
[$(A4)_5(D5)_2$]	2670	819705.9	31.3
[$(A6)_2(D2)_3$]	1602	491910.3	33.9
[$(A6)_4(D3)_4$]	3204	983944.4	40.8
[$(A6)_8(D4)_6$]	6408	1967641.2	47.7
[$(A6)_{20}(D5)_{12}$]	16020	4919474.4	76.8

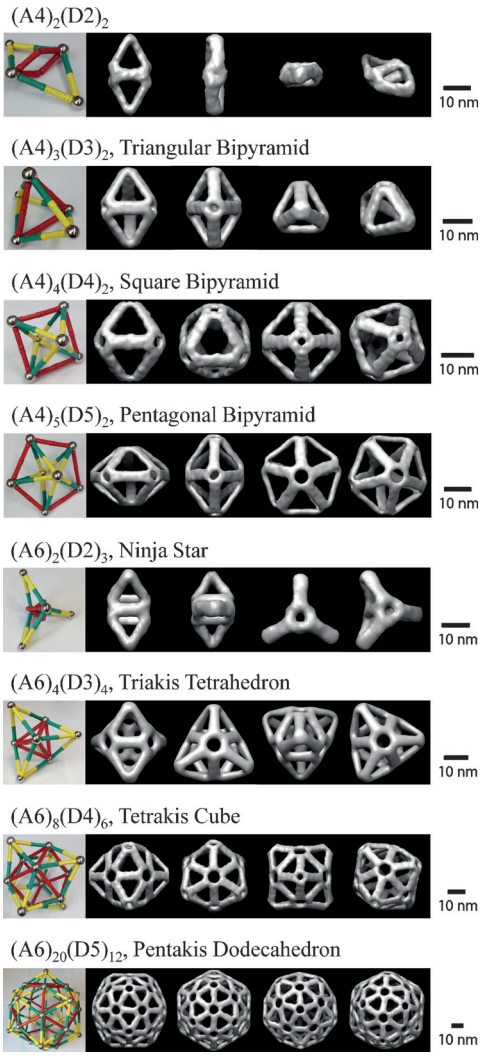

Figure 4. Reconstructed 3D structural models of the DNA complexes that resulted from directed self-assembly. For each structure, four views at different orientations are shown. The corresponding designs are shown on the left. See Figures S4–S17 for details.

Received: January 13, 2014
Published online: March 12, 2014

Keywords: cryogenic electron microscopy · DNA structures · nanocages · nanotechnology · self-assembly

[1] N. C. Seeman, *Annu. Rev. Biochem.* **2010**, *79*, 65 – 87.
[2] C. Lin, Y. Liu, S. Rinker, H. Yan, *ChemPhysChem* **2006**, *7*, 1641 – 1647.
[3] F. A. Aldaye, A. L. Palmer, H. F. Sleiman, *Science* **2008**, *321*, 1795 – 1799.
[4] E. Winfree, F. Liu, L. A. Wenzler, N. C. Seeman, *Nature* **1998**, *394*, 539 – 544.
[5] D. Liu, M. Wang, Z. Deng, R. Walulu, C. Mao, *J. Am. Chem. Soc.* **2004**, *126*, 2324 – 2325.
[6] P. W. K. Rothemund, A. Ekani-Nkodo, N. Papadakis, A. Kumar, D. K. Fygenson, E. Winfree, *J. Am. Chem. Soc.* **2004**, *126*, 16344 – 16352.
[7] J. C. Mitchell, J. R. Harris, J. Malo, J. Bath, A. J. Turberfield, *J. Am. Chem. Soc.* **2004**, *126*, 16342 – 16343.
[8] Y. He, Y. Chen, H. Liu, A. E. Ribbe, C. Mao, *J. Am. Chem. Soc.* **2005**, *127*, 12202 – 12203.
[9] H. Yan, *Science* **2004**, *306*, 2048 – 2049.
[10] S. Hamada, S. Murata, *Angew. Chem.* **2009**, *121*, 6952 – 6955; *Angew. Chem. Int. Ed.* **2009**, *48*, 6820 – 6823.
[11] M. N. Hansen, A. M. Zhang, A. Rangnekar, K. M. Bompiani, J. D. Carter, K. V. Gothelf, T. H. LaBean, *J. Am. Chem. Soc.* **2010**, *132*, 14481 – 14486.
[12] Y. He, T. Ye, M. Su, C. Zhang, A. E. Ribbe, W. Jiang, C. Mao, *Nature* **2008**, *452*, 198 – 201.
[13] J. Zheng, J. J. Birktoft, Y. Chen, T, Wang, R. Sha, P. E. Constantinou, S. L. Ginell, C. Mao, N. C. Seeman, *Nature* **2009**, *461*, 74 – 77.
[14] P. K. Lo, P. Karam, F. A. Aldaye, C. K. McLaughlin, G. D. Hamblin, G. Cosa, H. F. Sleiman, *Nat. Chem.* **2010**, *2*, 319 – 328.
[15] C. Zhang, W. Wu, X. Li, C. Tian, H. Qian, G. Wang, W, Jiang, C. Mao, *Angew. Chem.* **2012**, *124*, 8123 – 8126; *Angew. Chem. Int. Ed.* **2012**, *51*, 7999 – 8002.
[16] P. W. K. Rothemund, *Nature* **2006**, *440*, 297 – 302.
[17] Z. Zhao, H. Yan, Y. Liu, *Angew. Chem.* **2010**, *122*, 1456 – 1459; *Angew. Chem. Int. Ed.* **2010**, *49*, 1414 – 1417.
[18] D. Han, S. Jiang, A. Samanta, Y. Liu, H. Yan, *Angew. Chem.* **2013**, *125*, 9201 – 9204; *Angew. Chem. Int. Ed.* **2013**, *52*, 9031 – 9034.
[19] D. Han, S. Pal, Y. Yang, S. Jiang, J. Nangreave, Y. Liu, H. Yan, *Science* **2013**, *339*, 1412 – 1415.
[20] H. Dietz, S. M. Douglas, W. M. Shih, *Science* **2009**, *325*, 725 – 730.
[21] S. M. Douglas, H. Dietz, T. Liedl, B. Högberg, F. Graf, W. M. Shih, *Nature* **2009**, *459*, 414 – 418.
[22] D. Han, S. Pal, J. Nangreave, Z. Deng, Y. Liu, H. Yan, *Science* **2011**, *332*, 342 – 346.
[23] B. Wei, M. Dai, P. Yin, *Nature* **2012**, *485*, 623 – 626.
[24] Y. Ke, L. L. Ong, W. M. Shih, P. Yin, *Science* **2012**, *338*, 1177 – 1183.
[25] C. Mao, T. H. LaBean, J. H. Reif, N. C. Seeman, *Nature* **2000**, *407*, 493 – 496.
[26] P. W. K. Rothemund, N. Papadakis, E. Winfree, *PLoS Biol.* **2004**, *2*, 2041 – 2053.
[27] R. D. Barish, R. Schulman, P. W. K. Rothemund, E. Winfree, *Proc. Natl. Acad. Sci. USA* **2009**, *106*, 6054 – 6059.
[28] F. Zhang, Y. Liu, H. Yan, *J. Am. Chem. Soc.* **2013**, *135*, 7458 – 7461.
[29] S. Williams, K. Lund, C. Lin, P. Wonka, S. Lindsay, H. Yan, *DNA Computing*, *Lecture Notes in Computer Science*, *Vol. 5347* (Eds.: A. Goel, F. C. Simmel, P. Sosík), Springer, Berlin/Heidelberg, **2009**, pp. 90 – 101.
[30] Y. He, Y. Tian, Y. Chen, Z, Deng, A. E. Ribbe, C. Mao, *Angew. Chem.* **2005**, *117*, 6852 – 6854; *Angew. Chem. Int. Ed.* **2005**, *44*, 6694 – 6696.
[31] Y. He, Y. Tian, A. E. Ribbe, C. Mao, *J. Am. Chem. Soc.* **2006**, *128*, 15978 – 15979.
[32] C. Zhang, M. Su, Y. He, X. Zhao, P. Fang, A. E. Ribbe, W. Jiang, C. Mao, *Proc. Natl. Acad. Sci. USA* **2008**, *105*, 10665 – 10669.
[33] G. Tang, L. Peng, P. R. Baldwin, D. S. Mann, W. Jiang, I. Rees, S. J. Ludtke, *J. Struct. Biol.* **2007**, *157*, 38 – 46.
[34] T. D. Goddard, C. C. Huang, T. E. Ferrin, *J. Struct. Biol.* **2007**, *157*, 281 – 287.
[35] T. Briggs, A. M. Chandler, *Oklahoma Notes*: *Biochemistry* (Eds.: T. Briggs, A. M. Chandler), Springer, New York, **1995**, pp. 228.
[36] A. Patel, R. T. Noble, J. A. Steele, M. S. Schwalbach, I. Hewson, J. A. Fuhrman, *Nat. Protoc.* **2007**, *2*, 269 – 276.
[37] P. A. Thuman-Commike, B. Greene, J. A. Malinski, M. Burbea, A. McGough, W. Chiu, P. E. Prevelige, Jr., *Biophy. J.* **1999**, *76*, 3267 – 3277.
[38] B. A. Fane, P. E. Prevelige, Jr., *Adv. Protein Chem.* **2003**, *64*, 259 – 299.
[39] J. E. Johnson, *Curr. Opin. Struct. Biol.* **2010**, *20*, 210 – 216.

